Original Article
http://dx.doi.org/10.5115/acb.2014.47.3.162
pISSN 2093-3665 eISSN 2093-3673
Anatomy & Cell Biology acb

Effect of nicotine on the structure of cochlea of guinea pigs

Amel M. M. Abdel-Hafez, Sanaa A. M. Elgayar, Ola A. Husain, Huda S. A. Thabet
Department of Histology, Faculty of Medicine, Assiut University, Assiut, Egypt

Abstract: Smoking has been positively associated with hearing loss in human. However, its effect on the cochlea has not been previously evaluated. Aim of work is to investigate the effect of nicotine, which is the primary pharmacological component of tobacco, on the structure of the cochlea of adult male guinea pigs. Fifteen male guinea pigs were classified into two groups: group I (control) and group II (nicotine treated group). Group II was further subdivided into two subgroups; IIA and IIB according to the dose of nicotine (3 mg/kg and 6 mg/kg, respectively). The cochlea was harvested and processed for light microscopy, transmission electron microscopy and scanning electron microscopy. Nicotine administration induced damage of outer hair cells which were distorted in shape with vacuolated cytoplasm and heterochromatic nuclei. Topography revealed damage of the stereocilia which included disorganization, bent and limp or complete loss and expansion of the surrounding supporting cells. These changes were more pronounced in the basal turn of the cochlea and mainly involved the outer hair cells. High dose induced more damage and resulted in protrusion of the apical poles of hair cells (blebing), particularly the outer two rows. Nicotine is proved to be harmful to the cells of the cochlea, particularly the outer hair cells of the basal turn. High doses induce blebing of hair cells.

Key words: Nicotine, Cochlea, Guinea pigs, Scanning electron microscopy

Received May 28, 2014; Revised September 11, 2014; Accepted September 15, 2014

Introduction

Cigarette smoking is a major environmental health problem that is implicated in the development of many human diseases [1]. Nicotine is the primary pharmacological component of tobacco that acts on the brain and is believed to be the addictive tobacco agent [2]. In addition, therapeutic use of nicotine was suggested due to its anti-inflammatory effects [3] and antidepressant effects [4] in addition to it's neuroprotective effect in Parkinson's disease [5].

Smoking was reported to worsen the auditory thresholds at high frequencies and to increase the incidence of tinnitus, which is a frequent symptom in cochlear dysfunction [6]. Smoking has been positively associated with hearing loss in adults [7]. Sensory hearing loss occurs when there is damage to the cochlea, the end organ of hearing that lies deep within the temporal bone [8]. Inner hair cells (IHC) and outer hair cells (OHCs) are the sensory cells of hearing and they are very sensitive to harmful influences and toxic drugs [9]. The sensory hair cells are organized along with several types of supporting cells in an ordered pattern forming the organ of Corti with their apical surfaces joined together to form the reticular lamina [10]. The effect of nicotine on sensory hearing loss is unclear.

Therefore, the aim of this work, was to investigate the structural changes of the choclea that would be induced under the influence of nicotine administration in two different doses for the same duration on the structure of the cochlea of adult male guinea pigs. Using light microscopic,

Corresponding author:
Sanaa A. M. Elgayar
Department of Histology, Faculty of Medicine, Assiut University, Assiut 71515, Egypt
Tel: +20-1273636763, Fax: +20-88-2343703, E-mail: selgar1@hotmail.com

transmission electron microscopic (TEM) and scanning electron microscopic (SEM) techniques, the structure of the cochlea was evaluated after one month of nicotine exposure.

Materials and Methods

Materials

The drug

Nicotine hydrogen tartrate salt [1-methyl-2-(3-pyridyl) pyrrolidine-bitartrate salt] was purchased from Sigma-Aldrich (St. Louis, MO, USA). The drug was dissolved in physiological saline (0.9% sodium chloride) and injected subcutaneously.

The animals

The experimental animal selected was pigmented guinea pigs since they are easy to handle and the cochlea is easy to dissect. In addition, subcutaneous injection of nicotine is easily made in the nape of the neck [11]. A total number of 15 adult male pigmented guinea pigs that were 4 months age, 450–600 g body weight at the start of the experiment, were used in this study. The animals were housed in stainless steel cages under standard conditions (light, temperature and free access to food and water). Animal care and use were in accordance with procedures outlined in the National Institutes of Health Guidelines. The experiment was approved by the institutional ethics committee of Assiut University. The animals were divided into two groups:

Group I (control): This group included 5 animals that were injected subcutaneously with saline daily for one month.

Group II (nicotine treated): This group included 10 guinea pigs and was further subdivided into two equal subgroups, 5 animals each:

- Subgroup IIA: injected subcutaneously with nicotine dissolved in normal saline at a dose of 3 mg/kg body weight daily for one month
- Subgroup IIB: injected subcutaneously with nicotine dissolved in normal saline at a dose of 6 mg/kg body weight daily for one month

The nicotine doses (3 mg/kg and 6 mg/kg) were chosen to approximate the plasma levels reported in moderate and heavy smokers, respectively [12].

Methods

At the end of the experiment, the animals were anaesthetized with ether; their hearts were exposed and perfused through the left ventricle with glutaraldehyde cacodylate fixative. Each temporal bone with its tympanic cavity was removed by exposing the tympanic bulla and then opened for cochlear exposure. The labyrinths were promptly removed. The two cochleae of each animal were gently perfused with glutaraldehyde cacodylate fixative through an opening made on the cochlear apex. Then, the cochleae were put in the same fixative for one day.

The basal half of the left cochleae from all animals in group I and group IIA were used for transmission electron microscopy. Cochleae were decalcified in 4% EDTA in 0.1 M cacodylate buffer pH 7.3 for 48 hours. Then, the cochleae were rinsed in 0.1 M sodium cacodylate buffer several times before processing for TEM. Semithin sections (0.5–1 μm) were stained with toluidine blue (TB) and examined with light microscope [13]. Ultrathin sections (500–800A°) were cut, contrasted with uranyl acetate and lead citrate [14] and examined with the TEM JEOL (JEM-100 CXII, JEOL, Tokyo, Japan) and photographed at 80 KV in Assiut University-Electron Microscope Unit.

The right cochleae from animals of all groups were submitted to microdissection under a dissecting microscope in order to remove the bony wall of the cochleae and expose the membranous cochleae, whereas the tectorial membranes undergo retraction during processing. A graded series of alcohols was used for dehydration and liquid carbon dioxide was used to dry the specimens. Dried specimens were mounted on aluminum stubs and sputter coated with gold [15]. A SEM JEOL (J.S.M-5400 LV, Japanese Electron Optic Laboratory, Tokyo, Japan) was used to view the specimens. Photographs of the basal turn of the cochlea of each animal were taken at 15 KV.

Results

Light microscopy

In TB-stained semithin sections of control animals, the cell bodies of supporting cells rest on the basilar membrane which underlied the entire organ of Corti. The tectorial membrane appeared as a long spiral "blanket" which covered the organ of Corti. The long inner and outer pillars extended from the basilar membrane to the apical surface of the sensory epithelium (reticular lamina) enclosing the tunnel of Corti in between. Hensen's cells were located further laterally in the organ of Corti (Fig. 1). Semithin TB-stained sections of the

http://dx.doi.org/10.5115/acb.2014.47.3.162

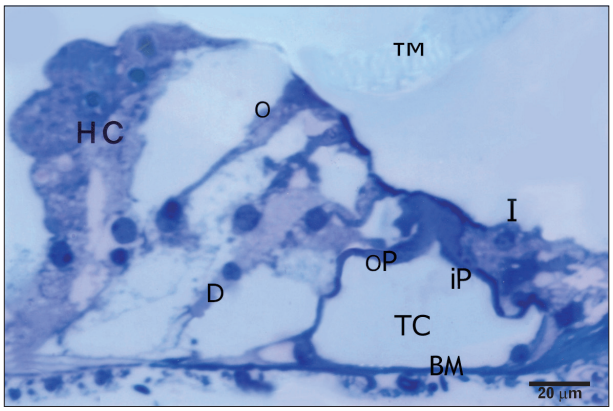

Fig. 1. Semithin section in the organ of Corti of group I, showing the normal organization of inner (I) and outer hair cells (O) and the surrounding supporting cells resting on the basilar membrane (BM). Note the tectorial membrane (TM), the inner (iP) and outer (oP) pillar cells enclosing the tunnel of Corti (TC), the Dieters' cells (D) and the laterally located Hensen's cells (HC) (toluidine blue staining, ×1,000).

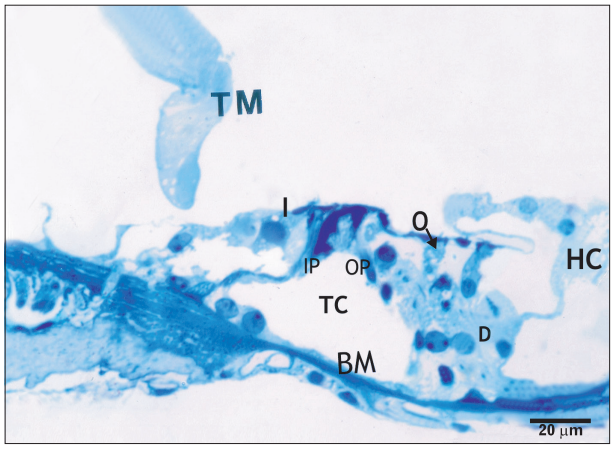

Fig. 2. Semithin section in the organ of Corti of group IIA, showing preservation of a relatively normal organization of the cells. The inner (I) and outer (O) hair cells have densely stained nuclei and vacuolated cytoplasm. Note the encroachment of Deiters' cells (D) toward the reticular lamina and Hensen's cells (HC) toward the piller cells. BM, basilar membrane; IP, inner piller; OP, outer piller; TC, tunnel of Corti; TM, tectorial membrane (toluidine blue staining, ×1,000).

organ of Corti of group IIA revealed that the IHCs and OHCs had densely stained nuclei and vacuolated cytoplasm. The Hensen's cells were disorganized and extended towards the pillar cell region (Fig. 2).

Transmission electron microscopy

In ultrathin sections of control animals, the OHCs characteristically revealed electron dense cuticular plate and graded height of straight stereocilia at their apical ends

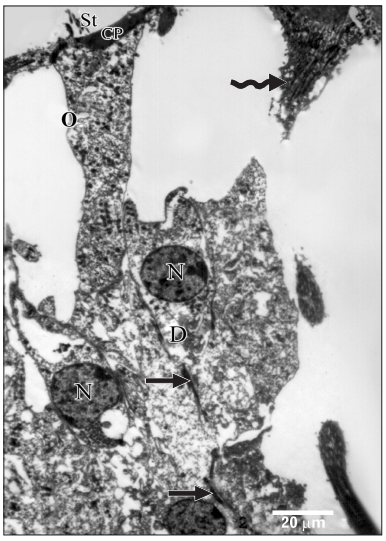

Fig. 3. Transmission electron microscopy of a portion of the organ of Corti of group I, showing the soma of an outer hair cells (O). Note the straight stereocilia (St) protruding from the cuticular plate (CP). Deiters' cells (D) have rounded nuclei (N) and microtubules running along their lateral plasma membrane (arrows) and surround their basal parts. Curved arrow, outer pillar (×2,900).

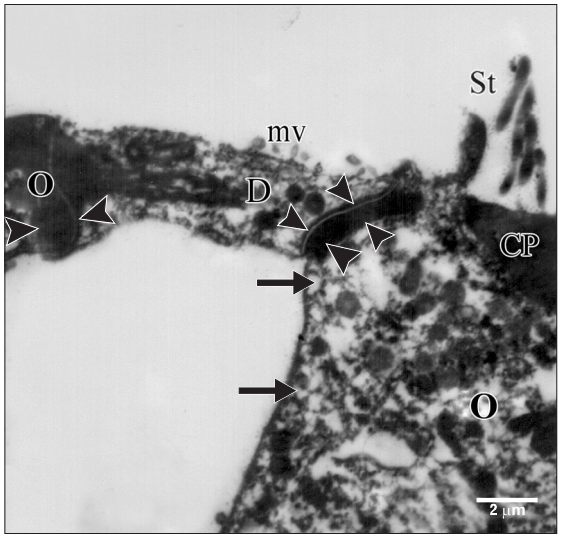

Fig. 4. Higher magnification of the previous figure showing the cuticular plate (CP), and the junctional complex (arrowheads) between the outer hair cell (O) and the Deiters' cell (D). Note the characteristic microfilament assembly appearing as electron dense structure running the depth of the junction and the subsurface cisternae (arrows) located under their lateral plasma membrane, stereocilia (St) and microvilli (mv) (×10,000).

and subsurface cisternae located under their lateral plasma membrane. The cell bodies of Deiters' cells, which had rounded heterochromatic nuclei and prominent bundles of

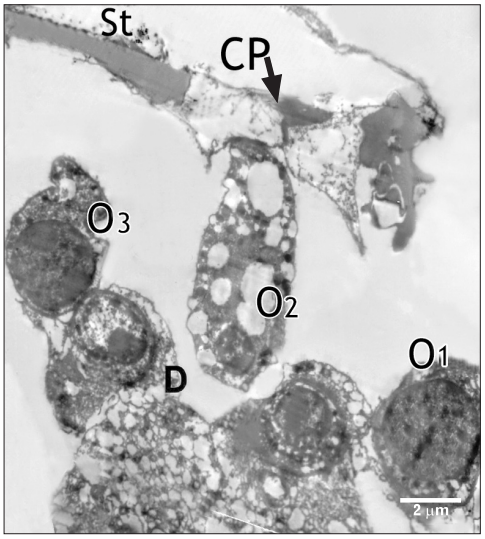

Fig. 5. Transmission electron microscopy from organ of Corti of group IIA, showing outer hair cells (O1, O2, O3) with vacuolated cytoplasm and wrinkled irregular lateral plasma membrane and heterochromatic nuclei. CP, cuticular plate; D, Deiters' cell; St, Stereocilia (×5,800).

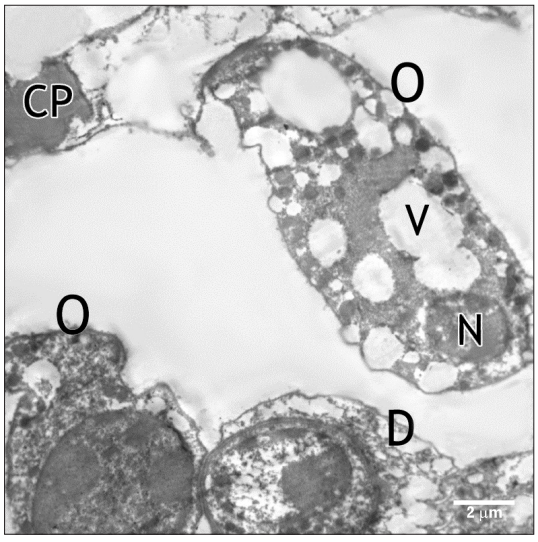

Fig. 6. High magnification of the previous figure showing the outer hair cells (O) heterochromatic nuclei (N), vacuolated cytoplasm (V) and dilated subsurface cisternae. A part of another hair cell shows electron dense nucleus with large heterochromatic clumps. CP, cuticular plate; D, Deiters' cell (×5,800).

microtubules running in their cytoplasm, enclosed the basal ends of OHCs and sent phalangeal processes (Figs. 3, 4). These processes expanded terminally at the reticular lamina where it formed junctional complex with the OHCs. These junctions were characterized by microfilament assembly appearing as electron dense structure running the depth of

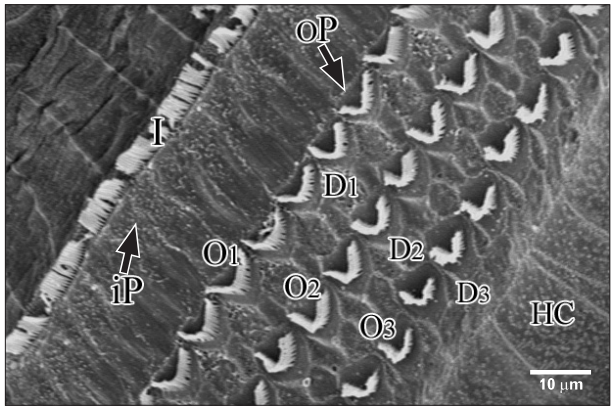

Fig. 7. Scanning electron microscopy of the organ of Corti (the reticular lamina) of group I. A single row of inner hair cells (I) is separated from the three rows of outer hair cells (O1, O2, O3), and the three rows of Deiters' cells (D1, D2, D3). HC, Hensen's cells; iP, inner pillar cells; oP, outer piller cells (×2,000).

the junction. The phalangeal processes of the outer pillar cells characteristically contained bundles of microtubules (Fig. 4). Ultrastructure of OHCs of group IIA showed distorted shape of their cell bodies with heterochromatic basal nuclei (Figs. 5, 6). In addition, subsurface cisternae appeared rounded or fused forming large vacuoles in the cytoplasm of OHCs (Fig. 6). Wrinkling and irregularity of the lateral plasma membrane were noticed in some OHCs. The Deiters' cells expanded upwards towards the reticular lamina (Fig. 5).

Scanning electron microscopy

The cochlea of control animals revealed the ordered cellular mosaic pattern made of the apical domains of hair cells and supporting cells in the organ of Corti which formed the reticular lamina. A single row of IHCs were separated from the three rows of OHCs by the apices of the inner pillar cells. Three rows of Deiters' cells were present between the OHCs. Hensen's cells were the outermost large cells positioned further laterally in the organ of Corti (Fig. 7). Each Deiters' cell is formed of the main cell body with its upper part forming a deep seat to enclose the basal portion of OHCs and its innervations. A phalangeal process extends from the Deiters' cell body towards the reticular lamina and terminates with an expansion (the head plate) which contributes to the reticular lamina by filling the spaces between OHCs (Fig. 8). IHCs and OHCs were characterized by tufts of stereocilia protruding from their apices. Stereocilia were cylindrical protrusions morphologically similar to large microvilli with granular appearance of their surface membrane. The tufts

http://dx.doi.org/10.5115/acb.2014.47.3.162

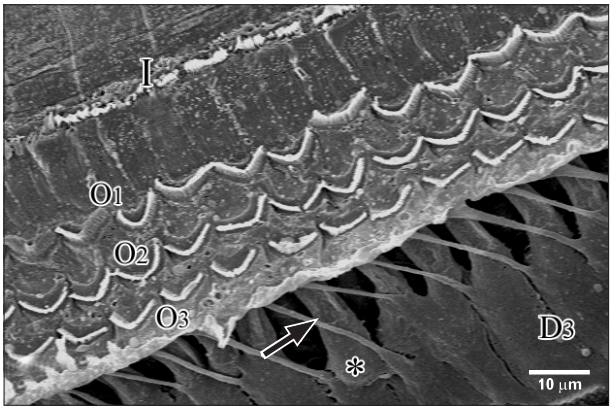

Fig. 8. Scanning electron microscopy of organ of Corti of group I. Hensen's cells are separated showing the cylindrical cell bodies of the third row of outer hair cells (asterisk) resting on the Deiters' cell bodies (D3). Note the phalangeal processes of Deiters' cells (↑) which extend obliquely to the reticular lamina. Outer hair cells (O1, O2, O3), inner hair cells (I) (×2,000).

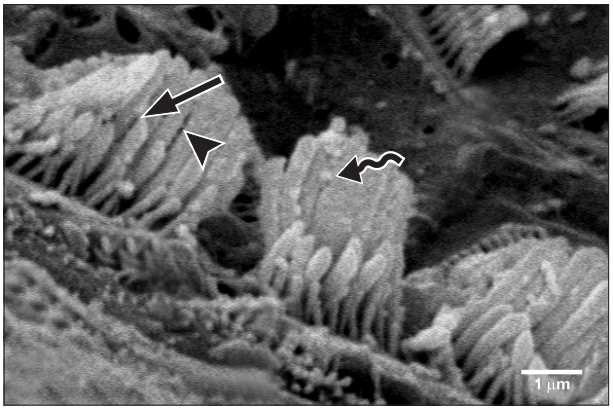

Fig. 9. Scanning electron microscopy of the inner hair cells of group 1, showing linear stereociliary bundles arranged in three rows of graded heights. Note the tip links (arrow) and side links (arrowhead) between stereocilia and the surface granularity of stereocilia (curved arrow) (×15,000).

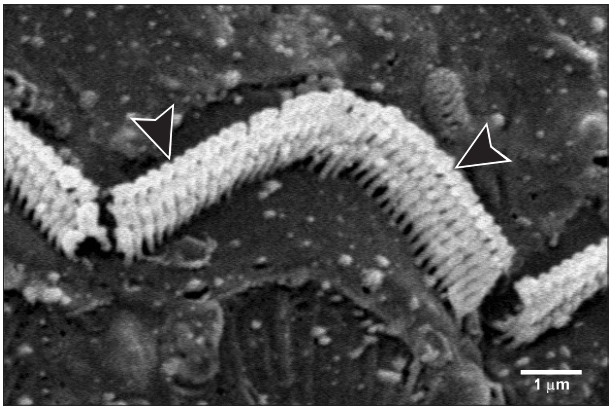

Fig. 10. Scanning electron microscopy of the outer hair cells of group I. The V-shaped stereociliary tufts are formed of three rows of stereocilia of graded height with the longest being in the outer side. Note the side links (arrowheads) between stereocilia (×15,000).

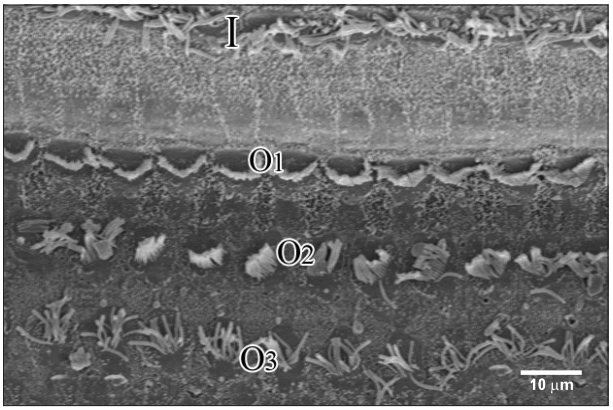

Fig. 11. Scanning electron microscopy of the reticular lamina of group IIA, showing disarray of the stereociliary bundles of the inner hair cells (I) and the outer hair cells particularly the third (O3) row (×2,000).

of stereocilia were mainly arranged in 3–4 rows with the shortest row seen on the inner aspect of the tuft. The apical tips of shorter stereocilia were connected diagonally to the sides of the adjacent taller stereocilia of the next row by thin filaments called tip links. Stereocilia in the same row were also connected to each other by side links. The stereocilia of IHCs formed a straight or gently curved bundles (Fig. 9), whereas, the OHC stereocilia formed a V-shaped pattern, with the tip of V directed externally (Fig. 10).

SEM of group IIA revealed that the surface changes of the cochlea were more noticeable in the basal turn of the cochlea. Although both types of hair cells were affected, the complete loss of the surface stereocilia was more prevalent in the OHCs than the IHCs (Figs.11–13). Some IHCs revealed disorganization of the tufts of stereocilia and loss of their links (Figs. 11, 12). Stereocilia on the apical surfaces of many OHCs revealed disordering of their regular arrangement and grouping into tufts. Individual stereocilia were bent at their bases and appeared separated from neighboring stereocilia with loss of tip and side links. Other OHCs showed complete loss of stereocilia leaving only a linear group of short stumps remaining on their apices. These changes were more obvious in the outer two rows of OHCs (Figs. 11, 13). Occasionally, complete loss of OHCs was observed with expansion of the apical poles of the surrounding supporting cells, forming "phalangeal scars" (Fig. 13).

In group IIB, the most characteristic change observed

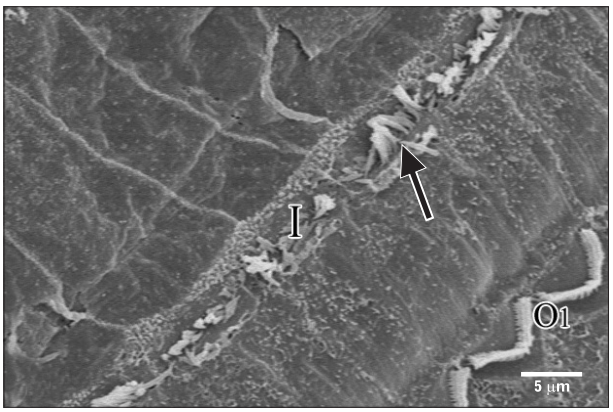

Fig. 12. Scanning electron microscopy of the reticular lamina of group IIA. The stereocilia protruding from the apices of inner hair cells (I) are bent and separated from each other with loss of their links (arrow). Note the relatively normal arrangement of stereocilia in the first row (O1) of outer hair cells (×7,500).

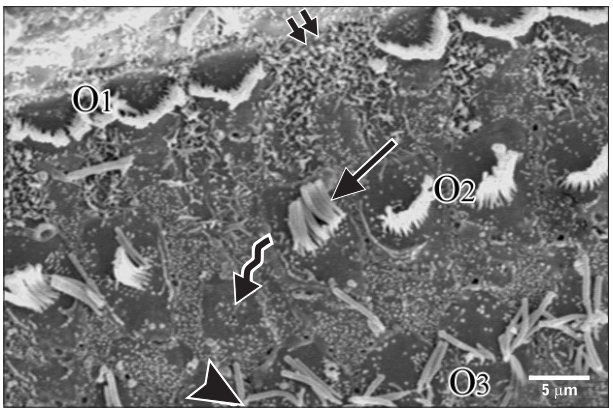

Fig. 13. Scanning electron microscopy of the reticular lamina of group IIA, showing the three rows of outer hair cells (O1, O2, O3). The stereocilia in O2 & O3 are bent (arrow), separated (arrowhead) or lost (curved arrow). Note the phalangeal scar extending from Deiters' cells in the site of lost outer hair cell (double arrow) (×2,000).

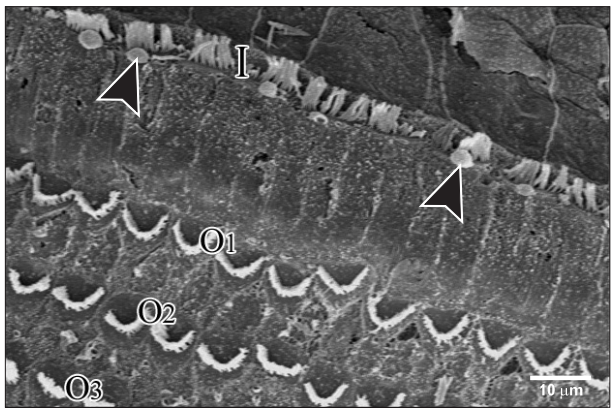

Fig. 14. Scanning electron microscopy of the reticular lamina of group IIB, showing frequent large blebs (arrowheads) arising from the cuticular plates of inner hair cells (×2,000).

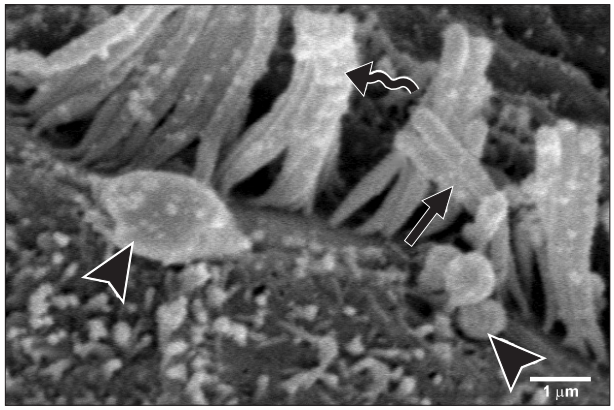

Fig. 15. Scanning electron microscopy of the inner hair cell row of group IIB, showing blebs with granular surfaces of varying size (arrowheads). Note the disarray (arrow) and increased surface granularity (curved arrow) of the stereocilia (×15,000).

in SEM of the organ of Corti of this group was the frequent detection large blebs with granular surfaces. The blebs appeared as balloon-like protrusions emerging from the cuticular plates of many IHCs and OHCs (Figs. 14–18). Disarray and loss of the regular arrangement of stereociliary bundles with increased surface granularity of the stereocilia were observed on many IHCs in the IHC row (Figs. 14, 15). In the OHC rows, stereociliary distortion and disarrangement were frequently noticed. Many OHCs revealed degeneration of the tufts of stereocilia with loss of stereociliary bundles. Complete loss of hair cells and expansion of surrounding supporting cells forming phalangeal scars were frequently observed (Figs. 16–18).

Discussion

The present work demonstrated the deleterious effect of nicotine on the OHCs which revealed distorted shape, heterochromatic nuclei and vacuolated cytoplasm. The apoptotic changes of the nuclei coincide with the result of Berger et al. [16] who reported that activation of nicotinic acetylcholine receptors by low doses of nicotine induces neuronal apoptosis. The OHCs have nicotinic acetylcholine receptors which are activated by the neurotransmitter acetylcholine [17]. The appearance of cytoplasmic vacuoles could be due to dilatation and fusion of subsurface cisternae which would result in wrinkling of the plasma membrane and distortion of the shape of the hair cell body. In support with this suggestion, the subsurface cisternae are supposed

http://dx.doi.org/10.5115/acb.2014.47.3.162

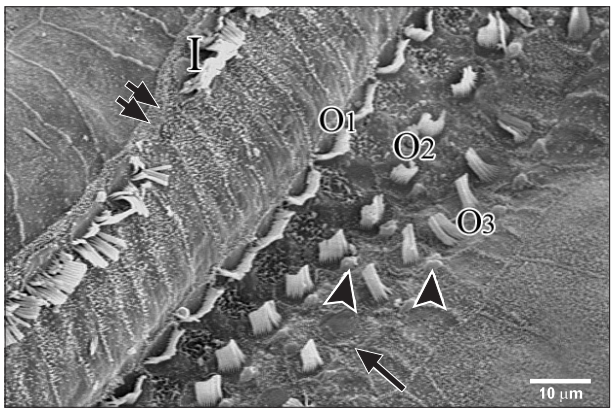

Fig. 16. Scanning electron microscopy of the reticular lamina of group IIB showing a phalangeal scar (double arrow) in the inner hair cell (I). Note the lost stereocilia (arrow) and the frequent blebs (arrowheads) (×2,000).

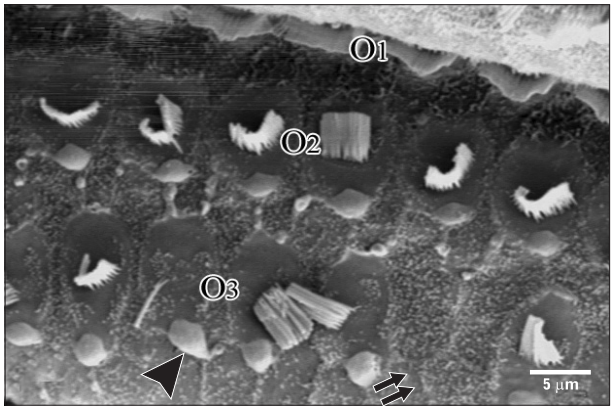

Fig. 17. Scanning electron microscopy of the reticular lamina of group IIB showing the three rows (O1, O2, O3) of outer hair cells with a phalangeal scar (double arrow) in the third row and the frequent blebs (arrowhead) (×3,500).

to maintain the cylindrical shape of OHC by stiffening its surface [18].

The phalangeal scars that we occasionally observed in topography of nicotine treated cochlea could be correlated with our findings in TEM which revealed the expansion of Deiters' cells upwards towards the reticular lamina. These findings coincide with those reported by previous workers in adult and young mammalian aminoglycoside ototoxicity [19]; in response to hair cell loss [9]. According to these authors the supporting cells (Deiters' and pillar cells) adjacent to the missing hair cells expanded and form these permanent epithelial scars. The developing expansions from Deiters' and pillar cells fill the spaces previously occupied by the missing hair cells and adopt various shapes resulting in the formation

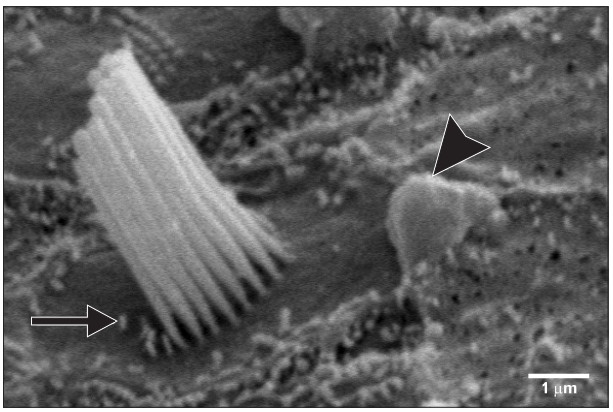

Fig. 18. Scanning electron microscopy at higher magnification showing a bleb and the stumps of the lost stereocilia (arrow) (×15,000).

of a disordered cellular mosaic appearance over the reticular lamina.

Hensen's cells have also been observed in this work by light and TEM closing in, on the pillar cells. In accordance with our finding, Taylor et al. [20] reported that with the loss of hair cells, the supporting cells are stimulated to change their shape together with an inward migration of cells from the outer edges of the organ of Corti strip. This would make Hensen's cells get closer to the pillar cell region, thus remodeling the structure of organ of Corti after hair cell loss [20].

Nicotine administration induced stereociliary changes as being bent and/or disorganized with a consequent loss of their tip and side links. Stereocilia are membrane bound cellular projections at the apical surface of hair cells that contain a dense core of actin filaments along with actin-associated proteins [21]. It has been known that the V-shape of the rows of stereocilia on the OHCs and the straight-line arrangement on IHCs were both appropriate for a maximal sensitivity of the hair cells to deflection of the stereocilia in a radial direction [22]. The staircase-shaped stereocilia bundles of the hair cells detect mechanical stimuli by the activation of mechano-electrical transduction channels at the stereocilia tips [23]. Also, the tip links and side links between adjacent stereocilia on the hair cell were reported to be important for sensory transduction [22]. Actin depolymerization of the stereocilia was hypothesized to account for hearing loss [24]. The malformation in the sensory hair cells and their stereocilia would consequently lead to clinical auditory impairment as recorded in human [18], in students [25] and in experimental animals as guinea pigs [24].

Topography of the hair cells revealed that nicotine induced hair cell damage in the basal turn of the cochlea of guinea

pigs with more affection of the OHCs. The use of high dose of nicotine, for the same period of time, exacerbates the structural changes. In support with our findings, loss and degeneration of OHCs were thought to be the most common form of cochlear damage that underlie most cases of mild to moderate sensory hearing loss [26]. OHCs are responsible for the motion of the basilar membrane through rapid and slow contractions, thus producing cochlear amplification [27]. It has been reported that diffuse damage of up to 30% of OHCs may occur without detectable hearing loss [28]. Smokers were found to have a higher prevalence rate of tinnitus [6], which was thought to be caused by OHC injury [29] whereas severe to profound sensory hearing loss included loss of OHCs and IHCs [30].

The balloon-like protrusions (blebs) of the apical plasma membrane have been observed in this work in relation to IHCs and/or OHCs by SEM. Similar findings have been previously noticed in cisplatin-treated guinea pigs [31] and following loud auditory stimulation [32]. Being noticed in relation to the IHC in an *in vitro* isolated organ of Corti of adult guinea pigs [33], these authors considered these blebs as physiological features arising as a result of an imbalance of endocytosis and exocytosis in the apical plasma membrane, linked to Na^+ loading which occurs *in vitro* [33]. On the other hand, they have been proposed to be an early degenerative change that develops when actin attachments between the plasma membrane of the hair cell and the underlying cytoskeleton were weakened [31]. Since these blebs were characteristically observed in this work following the use of high dose of nicotine they could be as an association with apoptotic hair cell injury as suggested by [34].

Our work revealed that the deleterious effect of nicotine involved mainly the basal turn of cochlea, which is the region where higher sound frequencies are transduced [35]. This finding could be correlated with the clinical findings that smoking increases the risk for high frequency hearing loss (at 4 kHz) in a dose dependent manner, whereas low frequency hearing loss (at 1 kHz) remained unchanged [36]. In addition, long term smoking with noise exposure was reported to be at a greater risk for developing a permanent hearing loss at high frequencies (3–4 kHz) than nonsmokers [37]. More recently, Paschoal and Azevedo [6] reported that the effects of smoking involved the most basal portion of the cochlea, affecting high sound frequencies permanently and progressively.

In conclusion, nicotine-induced structural damage of sensory hair cells involves mainly the basal cochlear turn and the outer rows in particular. Blebing of the outer plasma membrane of the hair cells occurs as an association with hair loss following the use of high dose of nicotine.

References

1. Cunningham CS, Javors MA, McMahon LR. Pharmacologic characterization of a nicotine-discriminative stimulus in rhesus monkeys. J Pharmacol Exp Ther 2012;341:840-9.
2. Hiremagalur B, Sabban EL. Nicotine elicits changes in expression of adrenal catecholamine biosynthetic enzymes, neuropeptide Y and immediate early genes by injection but not continuous administration. Brain Res Mol Brain Res 1995;32:109-15.
3. Ingram JR, Routledge P, Rhodes J, Marshall RW, Buss DC, Evans BK, Feyerabend C, Thomas GA. Nicotine enemas for treatment of ulcerative colitis: a study of the pharmacokinetics and adverse events associated with three doses of nicotine. Aliment Pharmacol Ther 2004;20:859-65.
4. McClernon FJ, Hiott FB, Westman EC, Rose JE, Levin ED. Transdermal nicotine attenuates depression symptoms in non-smokers: a double-blind, placebo-controlled trial. Psychopharmacology (Berl) 2006;189:125-33.
5. Quik M, Perez XA, Bordia T. Nicotine as a potential neuroprotective agent for Parkinson's disease. Mov Disord 2012;27:947-57.
6. Paschoal CP, Azevedo MF. Cigarette smoking as a risk factor for auditory problems. Braz J Otorhinolaryngol 2009;75:893-902.
7. Vinay. Effect of smoking on transient evoked otoacoustic emissions and contralateral suppression. Auris Nasus Larynx 2010;37:299-302.
8. Slepecky NB. Structure of the mammalian cochlea. In: Dallos P, Popper AN, Fay RR, editors. The Cochlea. New York: Springer; 1996. p.44-129.
9. Daudet N, Vago P, Ripoll C, Humbert G, Pujol R, Lenoir M. Characterization of atypical cells in the juvenile rat organ of corti after aminoglycoside ototoxicity. J Comp Neurol 1998;401:145-62.
10. Santi PA, Tsuprun VL. Cochlear microanatomy and ultrastructure. In: Jahn AF, Santos-Sacchi J, editors. Physiology of the Ear. San Diego: Singular Publishing; 2001. p.257-81.
11. Hyppolito MA, de Oliveira AA, Lessa RM, Rossato M. [Amifostine otoprotection to cisplatin ototoxicity: a guinea pig study using otoacoustic emission distortion products (DPOEA) and scanning electron microscopy]. Braz J Otorhinolaryngol 2005;71:268-73.
12. Matta SG, Balfour DJ, Benowitz NL, Boyd RT, Buccafusco JJ, Caggiula AR, Craig CR, Collins AC, Damaj MI, Donny EC, Gardiner PS, Grady SR, Heberlein U, Leonard SS, Levin ED, Lukas RJ, Markou A, Marks MJ, McCallum SE, Parameswaran N, Perkins KA, Picciotto MR, Quik M, Rose JE, Rothenfluh A, Schafer WR, Stolerman IP, Tyndale RF, Wehner JM, Zirger JM. Guidelines on nicotine dose selection for in vivo research.

http://dx.doi.org/10.5115/acb.2014.47.3.162

Psychopharmacology (Berl) 2007;190:269-319.
13. Gupta PD. Ultrastructural study on semithin section. Sci Tools 1983;30:6-7.
14. Reynolds ES. The use of lead citrate at high pH as an electron-opaque stain in electron microscopy. J Cell Biol 1963;17:208-12.
15. Albuquerque AA, Rossato M, Oliveira JA, Hyppolito MA. Understanding the anatomy of ears from guinea pigs and rats and its use in basic otologic research. Braz J Otorhinolaryngol 2009;75:43-9.
16. Berger F, Gage FH, Vijayaraghavan S. Nicotinic receptor-induced apoptotic cell death of hippocampal progenitor cells. J Neurosci 1998;18:6871-81.
17. Matsunobu T, Chung JW, Schacht J. Acetylcholine-evoked calcium increases in Deiters' cells of the guinea pig cochlea suggest alpha9-like receptors. J Neurosci Res 2001;63:252-6.
18. Dodson HC, Bannister LH, Douek EE. The effects of combined gentamicin and white noise on the spiral organ of young guinea pigs. A structural study. Acta Otolaryngol 1982;94:193-202.
19. Forge A. Outer hair cell loss and supporting cell expansion following chronic gentamicin treatment. Hear Res 1985;19:171-82.
20. Taylor RR, Jagger DJ, Forge A. Defining the cellular environment in the organ of Corti following extensive hair cell loss: a basis for future sensory cell replacement in the Cochlea. PLoS One 2012;7:e30577.
21. Pickles JO, Comis SD, Osborne MP. Cross-links between stereocilia in the guinea pig organ of Corti, and their possible relation to sensory transduction. Hear Res 1984;15:103-12.
22. Comis SD, Pickles JO, Osborne MP. Osmium tetroxide post-fixation in relation to the crosslinkage and spatial organization of stereocilia in the guinea-pig cochlea. J Neurocytol 1985;14:113-30.
23. Ricci AJ, Kachar B, Gale J, Van Netten SM. Mechano-electrical transduction: new insights into old ideas. J Membr Biol 2006;209:71-88.
24. Horner KC, Cazals Y, Guieu R, Lenoir M, Sauze N. Experimental estrogen-induced hyperprolactinemia results in bone-related hearing loss in the guinea pig. Am J Physiol Endocrinol Metab 2007;293:E1224-32.
25. Durante AS, Pucci B, Gudayol N, Massa B, Gameiro M, Lopes C. Tobacco smoke exposure during childhood: effect on cochlear physiology. Int J Environ Res Public Health 2013;10:5257-65.
26. Harpur ES, Bridges JB. An evaluation of the use of scanning and transmission electronmicroscopy in a study of the gentamicin-damaged guinea-pig organ of Corti. J Laryngol Otol 1979;93:7-23.
27. Brownell WE, Bader CR, Bertrand D, de Ribaupierre Y. Evoked mechanical responses of isolated cochlear outer hair cells. Science 1985;227:194-6.
28. Bohne BA, Clark WW. Growth of hearing loss and cochlear lesion with increasing duration of noise exposure. In: Harmernik RP, Handerson D, Salvi R, editors. New Perspective on Noise-Induced Hearing Loss. New York: Raven Press; 1987. p.208-302.
29. Hazell JW, Jastreboff PJ. Tinnitus. I: Auditory mechanisms: a model for tinnitus and hearing impairment. J Otolaryngol 1990;19:1-5.
30. Lenoir M, Puel JL. Dose-dependent changes in the rat cochlea following aminoglycoside intoxication. II. Histological study. Hear Res 1987;26:199-209.
31. Ramírez-Camacho R, García-Berrocal JR, Trinidad A, Verdaguer JM, Nevado J. Blebs in inner and outer hair cells: a pathophysiological hypothesis. J Laryngol Otol 2008;122:1151-5.
32. Zeddies DG, Siegel JH. A biophysical model of an inner hair cell. J Acoust Soc Am 2004;116:426-41.
33. Shi X, Gillespie PG, Nuttall AL. Na+ influx triggers bleb formation on inner hair cells. Am J Physiol Cell Physiol 2005;288:C1332-41.
34. Coleman ML, Sahai EA, Yeo M, Bosch M, Dewar A, Olson MF. Membrane blebbing during apoptosis results from caspase-mediated activation of ROCK I. Nat Cell Biol 2001;3:339-45.
35. Raphael Y, Altschuler RA. Structure and innervation of the cochlea. Brain Res Bull 2003;60:397-422.
36. Nakanishi N, Okamoto M, Nakamura K, Suzuki K, Tatara K. Cigarette smoking and risk for hearing impairment: a longitudinal study in Japanese male office workers. J Occup Environ Med 2000;42:1045-9.
37. Wild DC, Brewster MJ, Banerjee AR. Noise-induced hearing loss is exacerbated by long-term smoking. Clin Otolaryngol 2005;30:517-20.